Journal of Materials Chemistry B

Accepted Manuscript

ROYAL SOCIETY OF CHEMISTRY

www.rsc.org/materialsB

Water dispersible Ag@polyaniline-pectin as supercapacitor electrode for physiological environment

Chellachamy A. Amarnath,[a] Nandakumar Venkatesan,[b] Mukesh Doble,[b]

Shilpa N. Sawant[*,a]

[a] *Chemistry Division, Bhabha Atomic Research Centre, Trombay, Mumbai 400085, India.*

[b] *Department of Biotechnology, Indian Institute of Technology, Chennai, India.*

Correspondence: Email: stawde@barc.gov.in (Dr. Shilpa N. Sawant), Telephone: +22 25590288

Abstract: Designing the supercapacitor electrode material for implantable electronic medical devices (IEMDs) requires immense consideration because of the need for inherent material which has high capacitance, biocompatibility, antibacterial activity and ability to work under physiological environment. For the first time, we report the synthesis of a nanocomposite which has the above properties and have demonstrated as a supercapacitor electrode material operating in physiological fluids. In the first step, water dispersible polyaniline-pectin (PANI-PEC) nanoparticles have been synthesized using biopolymer pectin (PEC) as the stabilizer. In the second step, thus synthesized PANI-PEC was treated with silver nitrate solution to afford silver nanoparticles (Ag NPs) decorated PANI-PEC nanocomposite (Ag@PANI-PEC). PANI-PEC itself acted as a reducing agent to convert silver ions to Ag NPs eliminating the need of exogenous reducing agent. Ag@PANI-PEC displays specific capacitance of 140, 290, 144 and 121 F/g in physiological fluids like phosphate buffer saline, blood, urine and serum respectively. Furthermore, due to the use of biopolymer PEC, PANI-PEC and Ag@PANI-PEC exhibited biocompatibility and the presence of silver on Ag@PANI-PEC, rendered antibacterial property to the latter thus making them ideal material for *in vivo* implants. These findings establish the feasibility of using the nanocomposite as a potential material for energy storage device in IEMDs.

1. Introduction

Recently, there is a growing need for nanohybrid materials with unusual combination of properties to satisfy the challenges faced by modern biomedical science. [1] The late 20th century has been noticeable by the propagation of active implantable electronic medical devices (IEMDs). IEMDs comprise a broad range of products that include life-supporting implants like pacemakers, heart valves, cochlear implants, neurostimulators, and defibrillators and their use has been increased to sustain and improve the patient's health. The increase in production of IEMDs, have stimulated the increasing demand for high performance power sources like supercapacitor. Supercapacitors which store energy by separation of charges have fascinated unlimited curiosity over the past decade due to its high power density, low maintenance cost and long durability. [2] Generally, they are coupled with fuel cells or batteries to deliver high power in electrical energy storage and harvesting applications. The capacitance in supercapacitor originates either from the charging/discharging of the electrical double layers or from Faradic redox reactions. In the former case, the capacitance is derived from charge separation in the carbon-based materials and in the latter, a Faradic process takes place due to redox reactions in metal oxides or conducting polymers. The material properties required for an electrochemical capacitor include good electronic conductivity, chemical stability to alkaline and acidic electrolytes, low cost, and high specific surface area. [2] In addition to the above characteristics, supercapacitor for *in vivo* application needs to function under physiological conditions. The prerequisite to fabricate such devices are (i) to make use of material which is biocompatible with human body, (ii) to operate and sustain the device in physiological fluids, and (iii) to make the device with processable material. In the case of temporary implantation, the materials which are used for IEMDs could be easily removed after the purpose is served. However, these implantable

medical devices are linked with an ultimate peril of bacterial infection. [3] If the system has antibacterial property, it will be potentially useful for biomedical applications. [4, 5]

In recent decades, there has been a growing interest in the construction of supercapacitor electrodes with conducting polymer, especially PANI, due to its facile synthesis, redox property, tuneable morphology, inexpensive and better environmental stability as compared to other conducting polymers. [6] One of the major drawbacks of PANI is its poor solution processibility. Processible PANI can be synthesized using the sulfonic and dicarboxylic acid dopants. [6, 7] However, the PANI thus obtained is processable only in organic solvents which are not eco-friendly and thus the process is not easily acceptable for biological applications. The preparation of PANI dispersion is one of the ways to overcome this difficulty since colloidal dispersions can often be applied in place of true solutions. [8, 9] Water dispersible PANI can be prepared using many conventional water soluble polymer and biopolymer as stabilizers. [6, 10] Use of biopolymer as a stabilizer not only improves the processablity of PANI in water but also renders biocompatibility for potential biomedical applications. [11] Biopolymers have seldom been used with PANI for supercapacitor application due to their insulating and non-electroactive nature which consequently increases resistance of the electrodes. However, PANI or conducting polymers can be combined with carbon or metal oxides to demonstrate higher specific capacitance and stability. [12-14] Morphology of the electrode material also plays a vital role in enhancing specific capacitance. [15] In our previous research, we synthesized PANI nanorods and nanospheres on aniline primed indium tin oxide substrate and studied their morphology dependent supercapacitive property in which nanorods showed higher specific capacitance than nanspheres due to the availability of larger surface area for redox reactions. [16, 17]

To the best of our knowledge, researchers have used carbon, [18, 19] metal oxides, [20, 21] conducting polymers [22, 23] and their combinations [24-29] for supercapacitor application in acidic/basic/neutral aqueous or organic electrolytes. Supercapacitor operating in physiological fluids for application in IEMDs has seldom been reported. Recently, Malika and Jan modified PANI with multi wall carbon nanotubes on the stainless substrate and used as a supercapacitor electrode which can operate in physiological fluids. [30] Victor *et al*. demonstrated the design, fabrication, and packaging of flexible carbon nanotubes–cellulose based nanocomposite sheets, for energy storage application like supercapacitors, Li-ion batteries, and hybrids [31] in physiological fluids. However, the carbon nanotubes are not suitable for *in vivo* applications due to their potential toxicity. [32] Herein, for the first time, we demonstrate the synthesis of a supercapacitor electrode material with unusual combination of properties such as processability, electroactivity, biocompatibility, antibacterial property and ability to operate in physiological fluids. The conducting polymer, PANI has been modified by the biopolymer, PEC to obtain water dispersible PANI-PEC which was further treated with the $AgNO_3$ solution to form Ag NPs decorated PANI-PEC. The Ag@PANI-PEC exhibited satisfactory supercapacitive property in physiological fluids like PBS, blood, urine and serum.

2. Experimental section

Water dispersible PANI-PEC was synthesized by polymerization of aniline at room temperature in the presence of stabilizer PEC at various aniline:PEC w/w ratio (1:1, 1:2 and 1:3 and named as PP11, PP12, and PP13 respectively). Thus above prepared PANI-PEC was treated with 0.1 M $AgNO_3$ solution at 60°C to afford Ag NPs decorated PANI-PEC (Ag@PANI-PEC) and named as Ag111, Ag121, Ag131 respectively. To study the effect of $AgNO_3$ concentration on Ag@PANI-PEC synthesis, PANI-PEC (PP12) was treated with 0.05 M and 0.2 M $AgNO_3$

solution at 60^0C to afford Ag NPs decorated PANI-PEC which was named as Ag1205 and Ag122 respectively. PANI-PEC itself helped in reduction of silver ions to form Ag NPs, hence external reducing agent was not used. Working electrode for electrochemical characterization was prepared by casting known quantity of PANI-PEC or Ag@PANI-PEC dispersion on glassy carbon electrode (GCE). The details of synthesis, electrode preparation and characterization are given in ***supplementary information.***

3. Results and discussion

3.1 Synthesis of PANI-PEC

Water dispersible PANI-PEC was synthesized using various amounts of biopolymer PEC (1:1, 1:2 and 1:3 w/w of aniline:PEC) as a stabilizer. **Table S1** ***supplementary information*** shows the yield of the polymerization, amount of PEC present in the PANI-PEC and subsequent particle size when the amount of PEC was varied in the reaction mixture. The resulting PANI-PEC showed the average particle size 690±10 nm, 340±10 nm, 730±10 nm and polydispersity index (PDI) 0.52±0.05, 0.07±0.02, 0.59±0.03 respectively as analyzed by dynamic light scattering (DLS) measurement. The particle size of the PANI-PEC was higher in the case of 1:1 and 1:3 w/w of aniline:PEC due to the insufficient and excess coverage of PEC on the PANI particles respectively whereas 1:2 ratio gives highly uniform particle size (PDI=0.07). Insufficient amount of stabilizer PEC could cause macroscopic aggregation, because the π- π interaction between PANI particles overcomes the stabilizing capacity of PEC. At the same time, the excess amount of PEC on the PANI could forms gel like structure due to water absorption, swelling and consequently increases the particle size of PANI-PEC. This also reflects in the yield of polymerization as increasing the amount of PEC in the aniline polymerization increased the yield of polymerization (**Table S1**). During the synthesis, stability of the dispersion and electroactivity

of the product should be considered. The reasonable amount of PEC is essential on the surface of the PANI particles to keep the PANI-PEC dispersion stable without aggregation. On the other hand increasing the stabilizer amount decreases the electroactivity of the product due to the insulating and non-electroactive nature of stabilizer. In this situation, the PANI-PEC (PP13) synthesized using 1:3 aniline:PEC ratio is not suitable for the electrochemical studies. Keeping this in mind, the PANI-PEC synthesized using 1:2 aniline:PEC w/w (PP12) which could provide reasonable dispersion stability and electroactivity was considered as an optimum material for further studies. The PANI-PEC dispersion (**Fig. 1a**) prepared in our laboratory is stable over 8 months under normal atmospheric condition and we believe that it will be stable for at least one year duration without any macroscopic precipitation.

3.2 Synthesis of Ag@PANI-PEC

PANI-PEC in water was treated with $AgNO_3$ solution at 60 °C to afford water dispersible Ag NPs decorated PANI-PEC. Here, no additional reducing agent was required as PANI-PEC itself acted as a reducing agent to reduce Ag^+ ions to Ag^0 which adsorbed on to the surface of the PANI-PEC. In this experiment, the constant amount (in terms of concentration and volume) of PANI-PEC solution was used and the amount of $AgNO_3$ was varied (0.05 M to 0.2 M) to study the reduction effectiveness of PANI-PEC. The concentration of 0.1 M was found to be ideal because, at lower $AgNO_3$ concentration, there was no significant formation of Ag@PANI-PEC. Ag@PANI-PEC synthesized at higher $AgNO_3$ concentration was not dispersible in water which could be due to the aggregation of silver and PANI-PEC. In our previous work, PANI was used to reduce Au^+ ions to form PANI-Au nanocomposite which is insoluble in water and organic solvents. [33] Tamboli *et al*. synthesized PANI-Ag NPs using PANI as reducing agent and studied the antibacterial properties. [34] Our research group has earlier carried out biocompatibility studies

on PANI-Ag NPs nanocomposite where sodium citrate was used as the reducing agent. [35] Ivanova *et al*. synthesized pectin-Ag nanocomposite using pectin as a reducing agent. However, the reduction was carried out in presence of sodium hydroxide solution. [36] In the present work, the water dispersible PANI-PEC was used as a reducing agent to convert Ag^+ ions to Ag NPs on PANI-PEC which is dispersible in water (**Fig. 1b**). The hydroxyl groups in the PEC could facilitate inter- and intra-molecular hydrogen bonding to form supramolecular cages which allow the diffusion and reduction of Ag^+ ions in its vicinity. [37] In summary, PANI-PEC works as following: (i) a template for Ag^+ reduction and formation of Ag^0 on its surfaces, (ii) a green reducing agent, (iii) a stabilizer to protect the Ag^0 from aggregation, and (iv) a stabilizer to afford the dispersibility of Ag@PANI-PEC in water.

3.3 Characterization

3.3.1 Field emission-scanning electron microscopy (FE-SEM) analysis. The FE-SEM image of PANI-PEC (PP12) showed 'flattened rice' morphology with the length 150 nm and diameter 40 nm (**Fig. 1c and 1d**). The dimensions obtained from FE-SEM image are much lower as compared to the size obtained from DLS studies (340 nm). DLS study gives the average hydrodynamic radius of diffusing particles. PEC is known to swell to a large extent in aqueous medium, which could lead to a high hydrodynamic radius for PANI-PEC in dispersion. In the case of Ag@PANI-PEC (Ag121), the continuous growth of Ag NPs on the PANI-PEC shows the transition of flattened rice like morphology to nanocubes with the edge length about 75 nm (**Fig. 1e and 1f**). The EDX (electron dispersive X-ray spectroscopy) analysis indicates the presence of 15 % Ag in the particles (***supplementary information*** **Fig. S1**).

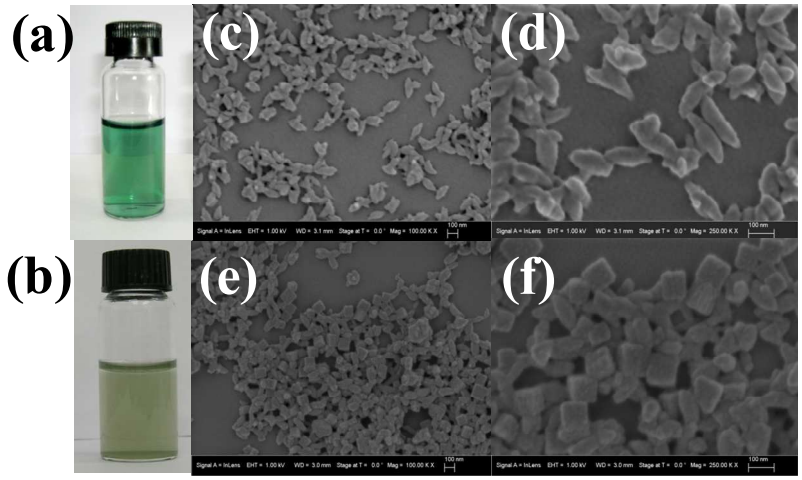

Fig. 1 Photographs of (a) PANI-PEC and (b) Ag@PANI-PEC dispersion in water; FE-SEM image of PANI-PEC (c and d) and Ag@PANI-PEC (e and f)

3.3.2 X-Ray Diffraction (XRD) analysis. Fig. 2a shows the XRD pattern of PANI-PEC (inset) and Ag@PANI-PEC. The diffractogram of PANI-PEC displayed two small humps around $2\theta = 20°$ and 25° which indicates the amorphous nature of the PANI-PEC. These are ascribed to periodicity parallel and perpendicular to the polymer chain respectively. [38] The XRD pattern of Ag@PANI-PEC (**Fig. 2a**) exhibits distinct diffraction peaks at 38.177º, 44.278º, 64.427º, 77.425º, and 81.539º which are indexed to (1 1 1), (2 0 0), (2 2 0), (3 1 1) and (2 2 2) planes of metallic silver, indicating a crystalline cubic structure (JCPDS file: 65-2871). The formation of Ag NPs on the PANI-PEC surface proves the efficiency of the PANI-PEC as a reducing agent.

3.3.3 Fourier Transform Infrared Spectroscopy (FTIR) analysis. The FTIR spectra for PANI-PEC and Ag@PANI-PEC are depicted in **Fig. 2b**. The spectra are complex and show a considerable broadening when compared to that of conventional PANI [10] which could be due to the various vibrations of PEC which has a complex polymeric structure. The broad band from 3640 cm^{-1} to 3300 cm^{-1} centred at 3420 cm^{-1} shows O-H stretching vibration from the PEC. The band at 2930 cm^{-1} is due to the asymmetric stretching of aliphatic C-H in PEC. The C=O stretching of carbonyl group of PEC and C=C stretching of quinoid rings of PANI, merges together to give broad peak centred at 1695 cm^{-1}. The peak at 1540 cm^{-1} and 1300 cm^{-1} shows the presence of C=C stretching vibration of benzenoid rings and C-N stretching in the PANI respectively. The peak related to the N=C=N bending vibration of PANI is shifted to lower wave number 1110 cm^{-1} from 1125 cm^{-1} which can be due to the hydrogen bonding between PEC and imine group of the PANI chains. [39]

3.3.4 UV-Visible spectroscopy analysis. UV-Visible spectrum of green colored PANI-PEC (**Fig. 2c**) displayed three peaks at around 330 nm (π–π^* transition in the benzenoid ring of PANI system), 430 nm (polaron to π^* transition in doped form of PANI) and 870 nm (π to polaron transition, signature of doped form of PANI system) which originate from electronic transitions characteristic of semi-oxidized protonated form of PANI. [10] The **Table S2** (***supplementary information***) shows the UV-visible spectroscopy data of PANI dispersion which are prepared using 1:1, 1:2, 1:3 aniline:PEC w/w. Increasing the amount of PEC stabilizer does not influence the PANI peak positions. The observance of bands in UV visible spectra of PANI-PEC proves its dispersibility in water. The PEC on the surface of PANI forms H-bonding with solvent water which leads to the higher degree of dispersibility of PANI-PEC.

UV–visible absorption spectrum of Ag@PANI-PEC is shown in **Fig. 2b**. Surface plasmon resonance is a vital optical property of nanoparticles and is illustrated as coherent fluctuations in electron density happening at a 'free electron' metal-dielectric interface. It is well-known that colloidal Ag NPs exhibit absorption at the wavelength from 390 to 420 nm due to Mie scattering. Generally, the polaron to π^* transition peak of the PANI system is also observes in this range (420-430 nm). The surface plasmon resonance peak of Ag and polaron to π^* transition peak of PANI were found to overlap, leading to a broad band in the 300 to 400 nm region in the case of Ag@PANI-PEC. [40]

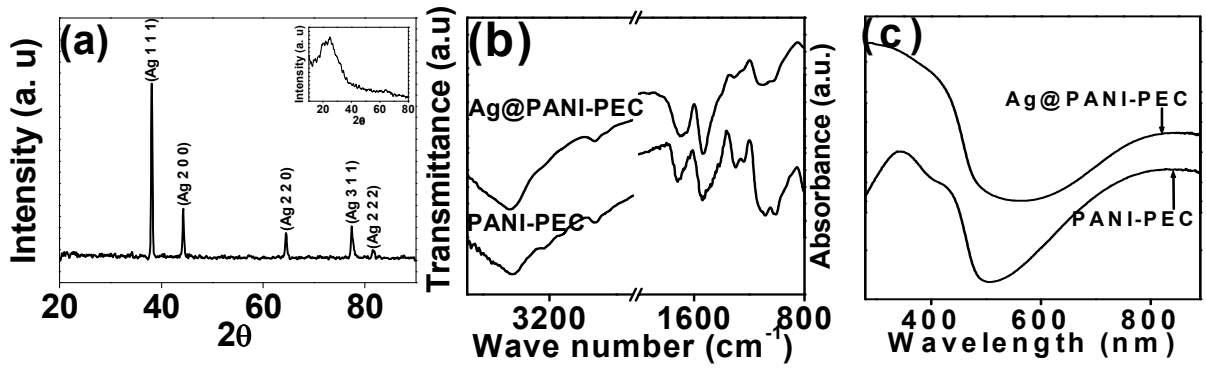

Fig. 2 (a) XRD pattern of Ag@PANI-PEC (Ag121) and PANI-PEC (PP12) (inset); (b) FTIR and; (c) UV-visible spectra of Ag@PANI-PEC (Ag121) and PANI-PEC (PP12).

3.3.5 X-ray Photoelectron Spectroscopy (XPS) analysis. N 1S XPS spectra of PANI-PEC and Ag@PANI-PEC are shown in **Fig. 3**. Generally, N 1S XPS spectra of PANI salt can be deconvoluted into three discrete curves at 398.2 eV, 399 eV, and 400 eV, associated to the quinoid imine, the benzenoid amine and positively charged nitrogen, respectively. [41] In present study, both the PANI-PEC and Ag@PANI-PEC displayed the three deconvoluted curves for N 1S which indicates the presence of PANI in protonated salt form. The N 1S deconvoluted peak

positions of PANI-PEC (399.0, 400.5 and 401.6 eV) and Ag@PANI-PEC (397.8, 398.6 and 399.6 eV) are slightly different from that of conventional PANI salt which could be due to the presence of PEC and Ag NPs in its system. The -NH-/-N= ratio of PANI-PEC is close to unity whereas for Ag@PANI-PEC the ratio is 0.2. This shows that the Ag@PANI-PEC contains more oxidized units (-N=) than the PANI-PEC which could be due to the oxidation of PANI by $AgNO_3$ which gets reduced to Ag NPs. The peak intensity of positively charged nitrogen ($-NH^+-$) in Ag@PANI-PEC is higher compared to the PANI-PEC. [40] 3d Ag XPS spectrum of Ag@PANI-PEC is shown in **Fig. 3**. The Ag species of Ag@PANI-PEC display two bands at around 368.3 and 374.2 eV, which can be ascribed to Ag $3d_{5/2}$ and Ag $3d_{3/2}$ binding energies, individually. [42]

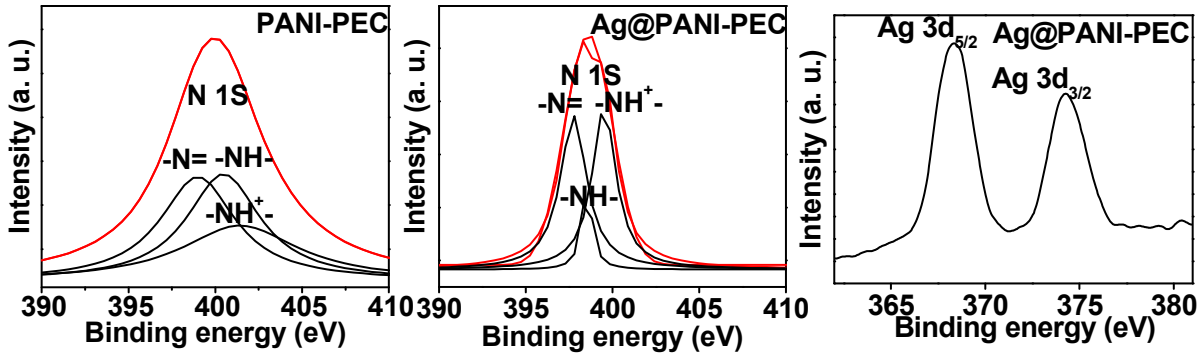

Fig. 3 N 1S XPS spectra of PANI-PEC (PP12) and Ag@PANI-PEC (Ag121); Ag 3d XPS spectra of Ag@PANI-PEC (Ag121).

3.3.6 Electrochemical Studies. In order to evaluate the feasibility of using Ag@PANI-PEC in IEMDs, its supercapacitive property was studied in physiological fluids. **Fig. 4a** depicts the CV of PANI-PEC, Ag@PANI-PEC, PEC, and bare GCE in PBS electrolyte at a scan rate of 100 mV s^{-1}. PANI-PEC did not display significant electroactivity, probably due to the insulating nature of PEC. CV of Ag@PANI-PEC showed higher current as compared to PANI-PEC which reflects its better electroactivity despite the presence of PEC as evidenced from FTIR studies.

The presence of Ag NPs helped to expedite electron transport by acting as a bridge between the GCE – PANI and PANI–electrolyte interfaces resulting in reasonable electroactivity in PBS. [43] **Fig. 4b** shows the CV of Ag@PANI-PEC at different scan rates (100, 50, 25, 5 mV/s) for a potential window of -0.1 to 1.0 V *vs* Ag/AgCl in PBS electrolyte. Rectangular shape CV was obtained demonstrating good charge propagation in the electrodes. It can be seen that CVs retained their shape even at a high scan rate, indicating that the Ag@PANI-PEC has rapid current response on voltage reversal. Even though PANI systems are recognized to display high pseudo-capacitance due to existence of numerous oxidation states, **Fig. 4** did not show the pseudo-capacitance behavior which might be due to the low proton concentration in the PBS electrolyte. The supercapacitive property of PANI-PEC and Ag@PANI-PEC electrodes in physiological fluids was assessed by conducting galvanostatic charge–discharge measurement at a constant current density of 1.5 A/g in the potential range between 0 and 0.9 V *vs* Ag/AgCl. The specific capacitance (C_{sp}) was calculated from the discharge curve according to the equation $C_{sp} = i/(m(\Delta V/\Delta t))$, where 'm' is mass of the active material in grams, 'i', the applied current in amperes, $\Delta V/\Delta t$ is slope of discharge curve. [44] Based on the above equation, the specific capacitance of PANI-PEC synthesized using 1:1, 1:2, 1:3 aniline:PEC w/w ratio was 25, 15 and 10 F/g respectively in PBS electrolyte at current density 1.5 A/g. Consequently, specific capacitance of Ag nanocomposites (Ag@PANI-PEC) which was prepared using above PANI-PEC samples was 40, 140, 37.5 F/g respectively in PBS electrolyte at current density 1.5 A/g respectively. A representative plot for the charge-discharge curve of PANI-PEC (synthesized using 1:2 aniline:PEC w/w ratio) and Ag@PANI-PEC (prepared using PANI-PEC which was synthesized using 1:2 aniline:PEC w/w ratio and 0.1 M $AgNO_3$ and named as also Ag121) is shown in **Fig. 5a**. To understand the influence of the amount of Ag NPs on the specific

capacitance, Ag@PANI-PEC was synthesized using different molar concentration of $AgNO_3$ (0.05 M, 0.2 M and named as Ag1205 and Ag122 respectively). Galvanostatic charge discharge studies for Ag1205 and Ag122 gave a specific capacitance of 25 and 135 F/g respectively (**Fig. 5b**). Lesser specific capacitance of Ag1205 could be due to the presence of insufficient amount of Ag NPs on the PANI-PEC. Charge-discharge cyclic stability is another important property for supercapacitors electrode material. The normalized capacitance (%) of Ag@PANI-PEC in PBS as a function of cycle number (current density of 2.5 A g^{-1}) is depicted in **Fig. S2a (*supplementary information*)**. The capacitance of the Ag@PANI-PEC was found to decrease sharply over 250 charge-discharge cycles, retaining 80 % of the initial value. After this, there was only 12 % loss from 250 to 1000 cycles retaining 68 % of initial capacitance (**Fig. S2a**). PANI is known to lose its electroactivity to a certain extent on continuous cycling, especially in solutions with high pH. [45] None-the-less, Ag@PANI-PEC exhibited satisfactory electroactivity and specific capacitance even after 1000 cycles due to the presence of Ag NPs. The stability can be further improved by operating the electrode in lower voltage range to avoid oxidation and decomposition of polyaniline. Hence, galvanostatic charge-discharge was carried out at 2.5 A g^{-1} in lower voltage range of 0 - 0.6 V Vs Ag/AgCl. In this case, there was only 5% loss over 250 cycles and at the end of 1000 cycles, 85 % of the initial capacitance was retained (**Fig. S2b)**. Thus depending on the type of application, the voltage range can be tuned to get desired capacitance and stability. In the view of above results, the Ag@PANI-PEC (prepared by PANI-PEC which was synthesized using 1:2 aniline:PEC w/w ratio and 0.1 M $AgNO_3$) which has reasonable specific capacitance 140 F/g was chosen for further studies in other physiological fluids like blood, urine and serum.

Fig. 6a shows the CV of Ag@PANI-PEC in PBS, blood, urine and serum supporting electrolytes at the scan rate 100 mV/s for the potential window -0.1 V to 1.0 V *vs* Ag/AgCl. As compared to PBS, the nature of CV in these electrolytes was found to be different due to the presence of complex components in these physiological fluids. Consequently, the specific capacitance of Ag@PANI-PEC in blood, urine, and serum at current density 1.5 A/g was found to be 290, 144, and 121 F/g respectively (**Fig. 6b**). The potential *vs* time plot in the charge-discharge experiment (**Fig. 6b**) is not an ideal 'inverted V' shaped curve (linear and typical triangular distribution) as expected in the case of electrical double layer capacitance. Generally, in the case of a pseudo-capacitance, slightly distorted 'inverted V' shape curve is observed due to the Faradic processes involved. The distortion in PBS, urine and serum are not much significant as compared o that in the case of blood, probably due to the complex composition of the latter.

Based on the electrochemical investigations, it can be summarized that Ag@PANI-PEC display reasonable specific capacitance in physiological fluids due to the synergistic effect of its components PANI and Ag NPs. The nano-sized morphology of Ag@PANI-PEC expedites ion diffusion from the electrolyte to electrode, making full utilization of the active materials. Moreover, the Ag NPs present on the surface of Ag@PANI-PEC facilitates the quick electron transfer from electrode to electrolyte by the bridging effect. The PEC present in Ag@PANI-PEC electrode could form supramolecular assemblies or nanocages on the surface of the electrode using inter and intramolecular H-bonding. These nanocages trap the electrolyte near the electrode surface and increase the interaction between electrode and electrolyte and hence provide high specific capacitance to the material despite of its insulating and non-electroactive nature. The nanocages on the surface also prevent the electrode material from shrinking during the intercalation/de-intercalation of the counter ions. [46, 47] These studies revealed that the

electroactivity of Ag@PANI-PEC in physiological fluids can be utilized for potential application in IEMDs.

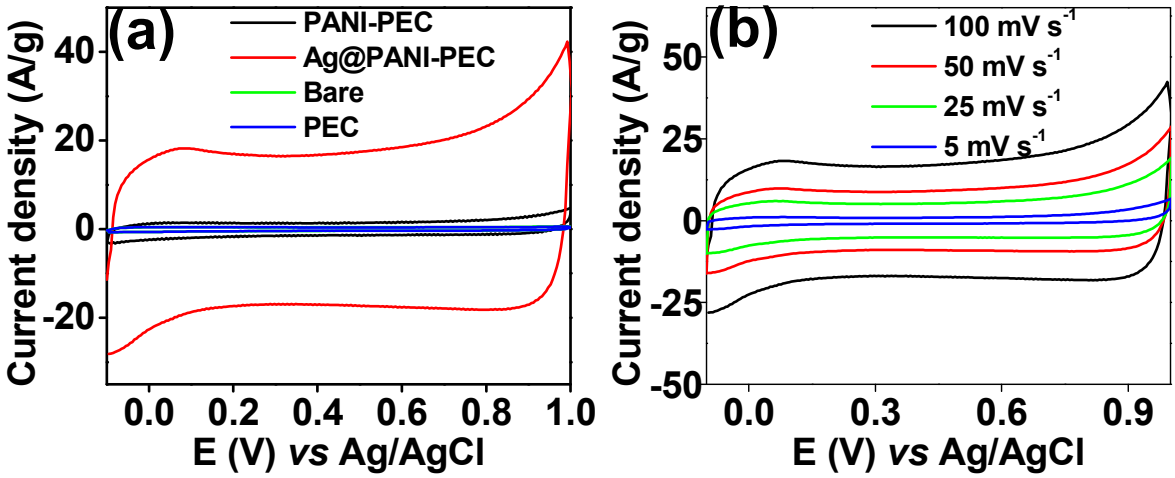

Fig. 4 CV in PBS from -0.1 to 1.0 V *vs* Ag/AgCl of (a) PANI-PEC (PP12), Ag@PANI-PEC (Ag121), Bare-GCE and PEC at 100 mV/s scan rate; (b) Ag@PANI-PEC (Ag121) at different scan rates 100, 50, 25, 5 mV/s.

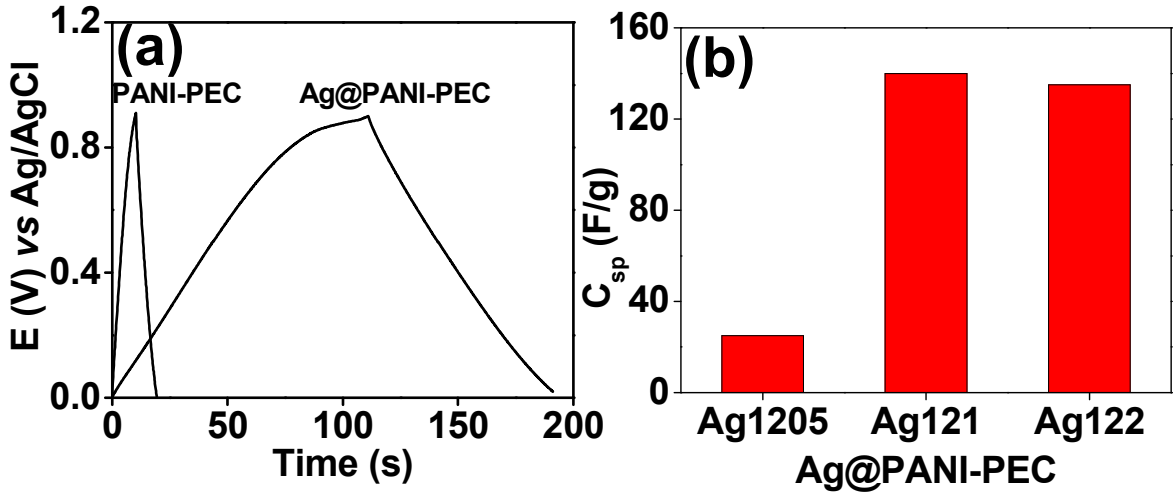

Fig. 5 (a) Galvanostatic charge-discharge curve of PANI-PEC (PP12) and Ag@PANI-PEC (Ag121), (b) C_{sp} of Ag@PANI-PEC which was prepared using different molar concentrations of $AgNO_3$.

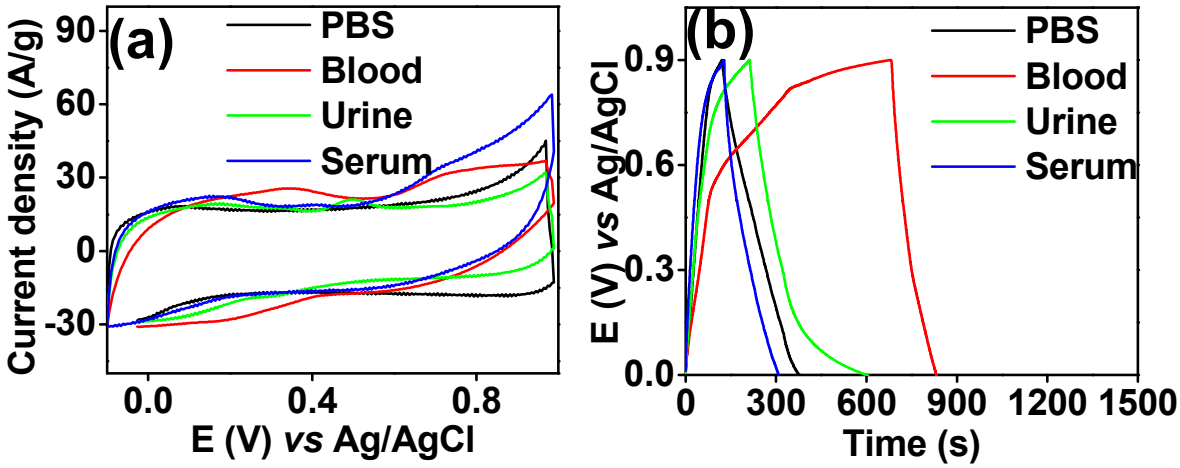

Fig. 6 (a) CV of Ag@PANI-PEC (Ag121) from -0.1 to 1.0 V *vs* Ag/AgCl in PBS, blood, urine and serum at scan rate of 100 mV/s; (b) Charge-discharge curve of Ag@PANI-PEC(Ag121) in PBS, blood, urine and serum at cut off voltage from 0 to 0.9 V *vs* Ag/AgCl

Generally, supercapacitor for IEMDs is less likely to come in direct contact with the tissue or blood as it will be packed well inside the device casing. However, in the case of malfunction of the casing, there is a probability of the supercapacitor material being exposed to the tissue/ blood. From this point of view, the biocompatibility and antibacterial studies have been carried out to analyze the safety of the material.

3.3.7 *In vitro* Biocompatibility of Polymer Films. The biocompatibility of polymer films was assessed with L6 rat myoblast cells and the cell viability was determined by MTT assay[48]. The percentage of viable cells was 83.16, 89.28, and 91.01% for PANI-PEC (**Fig. S3a** in ***supplementary information***) prepared using 1:1, 1:2, 1:3 aniline:PEC w/w. Viability of cells increased as PEC amount increased in the PANI-PEC. This is because PEC is a biopolymer and well established for its biocompatibility. On the other hand, the % cell viability of respective Ag

NPs decorated PANI-PEC nanoparticles was 94.41, 89.77, and 77.35 % (**Fig. S3b** in ***supplementary information***). Pectin acts as a mild reducing agent and favors the formation of Ag NPs. [36] It is reported that silver-PEC nanoparticles enhance the singlet oxygen production by 1.8 fold and induce selective damage to the tissues. [49] Higher concentration of PEC in our case could lead to higher formation of Ag NPs thus reducing the cell viability. When the concentration of $AgNO_3$ solution was varied (0.2 M, 0.1 M and 0.05 M), the resulting Ag@PANI-PEC exhibited 44.67, 89.77 and 87.18 % cell viability respectively (**Fig. S3c** in ***supplementary information***). There are several reports in literature on cytotoxicity associated with silver nanoparticles due to the presence of unconverted Ag^+ ions which are known to be toxic to the cells. [50] Hence, in the present work, the samples were washed with 1% ammonia solution to remove AgCl which resulted in improved biocompatibility. Based on these studies, it could be concluded that 0.1 M $AgNO_3$ is the optimum concentration required to afford nanocomposite with reasonable cell viability.

3.3.8 Bacterial adhesion assay. Adhesion of Gram negative *Escherichia coli* (NCIM 2931) was tested on polymer films. [48] The values of bacterial adhesion for the various samples of PANI-PEC and Ag@PANI-PEC are shown in **Table S3** in ***supplementary information***. The bacterial adhesion was found to increase with amount of PEC whereas with increase in amount of Ag NPs, it was found to drastically decrease which could be attributed to antibacterial property endowed by Ag NPs (**Fig S4** in ***supplementary information***). Here too, it was observed that the Ag@PANI-PEC prepared using 0.1 M $AgNO_3$ and PANI-PEC (synthesized using 1:2 w/w aniline:PEC) gave the optimum antibacterial property. The above results reveal that the biocompatible and antibacterial nature of PANI-PEC and Ag@PANI-PEC can be tuned

accordingly to the composition (and as per the application) and hence increases the feasibility of using these materials for *in vivo* application.

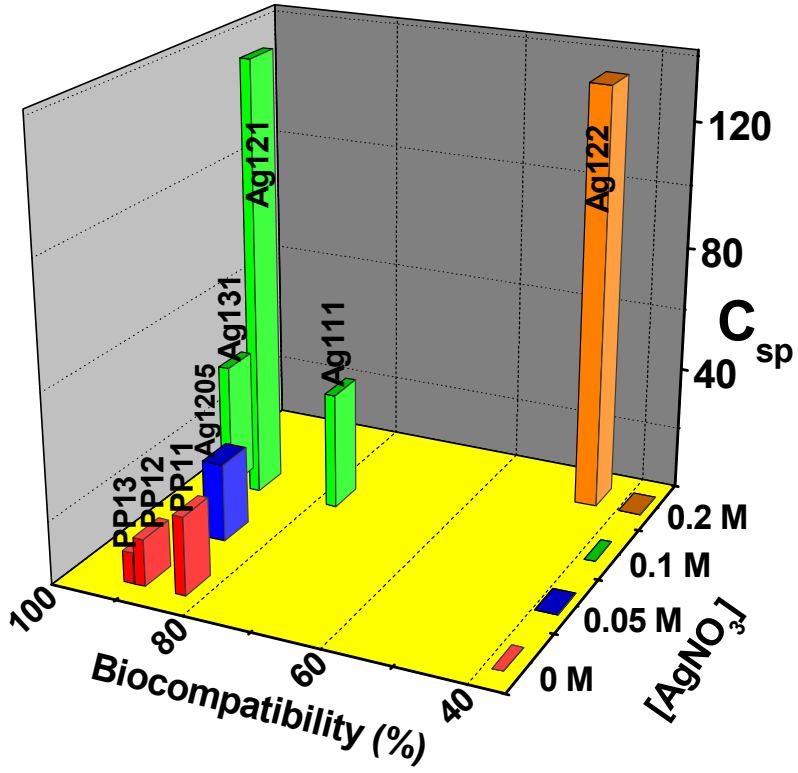

Fig. 7 Specific capacitance (F/g) and biocompatibility for the various PANI-PEC and Ag@PANI-PEC samples. [Abbreviations: PP11, PP12 and PP13 = PANI-PEC synthesized using different ratio of aniline:PEC w/w, (1:1, 1:2 and 1:3 respectively); Ag111, Ag121, Ag131 = Ag@PANI-PEC synthesized from PP11, PP12 and PP13 using 0.1M $AgNO_3$; and Ag1205, Ag121, Ag122 = Ag@PANI-PEC synthesized from PP12 using different concentrations of $AgNO_3$ (0.05M, 0.1M and 0.2M respectively)].

In the present work, four properties namely, (a) electroactivity or specific capacitance in physiological fluids, (b) biocompatibility, (c) antibacterial activity and (d) water dispersibility have been introduced in a single nanocomposite. The results of this study (**Fig 7, Fig.S5 and**

Table S3 in ***supplementary information***) can help to select an appropriate composition based on the envisaged application. Improving one property of the nanocomposite, could affect another property, hence an appropriate composite needs to be selected based on the requirement. Our research group is working on silver nanocomposites to further improve the electroactivity, biocompatibility and water dispersibility simultaneously.

4. Conclusions

To conclude, we demonstrate the synthesis of water dispersible nanocomposite Ag@PANI-PEC exhibiting electroactivity, specific capacitance (in physiological fluids) as well as reasonable biocompatibility and antibacterial property. The specific capacitance of Ag@PANI-PEC at current density 1.5 A/g was 140, 290, 144, and 121 F/g in PBS, blood, urine, and serum respectively. These results endorse that this nanocomposite may discover commercial potential for environmental friendly and inexpensive supercapacitor electrode in biomedical applications. Furthermore, the biocompatibility and antibacterial nature of the Ag@PANI-PEC endorse the feasibility of using it for *in vivo* applications. The forthcoming effort will emphasize on additional characterizations, reviewing the mechanism, and going with trials of *in vivo* implantation. Enhancing the electroactivity and biocompatibility of the nanocomposite is underway.

Supplementary Information

The details of materials, characterization techniques, PANI-PEC and Ag@PANI-PEC syntheses, electrode preparation and sample preparation for biocompatibility/bacterial adhesion studies are given in ***supplementary information.*** Additional experimental findings including the influence of pectin on the nanocomposite yield, Energy Dispersive X-ray spectroscopy (EDX) data of

Ag@PANI-PEC, UV-Visible spectral data of PANI-PEC, *In vitro* biocompatibility and antibacterial study of polymer films are also given. Table with sample description, synthesis condition, values of specific capacitance (C_{sp}), % cell viability (biocompatibility), and bacterial adhesion (antibacterial activity) is given.

Acknowledgements

CAA is grateful to BRNS, Department of Atomic Energy for providing KSKRA fellowship. Authors are thankful to Dr. C. B. Basak and Dr. M. Krishnan (for FE-SEM measurements), Dr. Jagannath (for XPS measurements), Mr. J. Nuwad (for EDX measurement), Ms. J. A. Prabhu and Mr. S. D. Kamble (for providing blood, urine, and serum samples) from BARC for their support during this work.

Notes and references

1. C. A. Amarnath, S. S. Nanda, G. C. Papaefthymiou, D. K. Yi and U. Paik, *Crit. Rev. Solid State Mater. Sci*., 2013, **38**, 1.

2. A. Burke, *J. Power Sources*, 2000, **91**, 37.

3. M. Jamal, F. M. Shaikh, B. Aslam and K. M. Razeeb, *Anal. Methods*, 2012, **4**, 1865.

4. I. Mahapatra, J. Clark, P. J. Dobson, R. Owen and J. R. Lead, *Environ. Sci.: Processes Impacts*, 2013, **15**, 123.

5. M. C. C. Ferrer, N. J. Hickok, D. M. Eckmann, and R. J. Composto, *Soft Matter*, 2012, **8**, 2423.

6. S. Bhadra, D. Khastgir, N. K. Singha, and J. H. Lee, *Prog. Polym. Sci*., 2009, **34**, 783.

7. S. Palaniappan, and C. A. Amarnath, *React. Funct. Polym*., 2006, **66**, 1741.

8. M. Aldissi, *Adv. Mater*., 1993, **5**, 60.

9. S. P. Armes and M. Aldissi, *J. Chem. Soc., Chem. Commun*.**,** 1989, 88.

10. C. A. Amarnath, S. Palaniappan, P. Rannou and A. Pron, *Thin Solid Films*, 2008, **516**, 2928.

11. M. Li, Y. Guo, Y. Wei, A. G. MacDiarmid, and P. I. Lelkes, Biomater., 2006, **27**, 2705.

12. Z. Niu, P. Luan, Q. Shao, H. Dong, J. Li, J. Chen, D. Zhao, L. Cai, W. Zhou, X. Chen and S. Xie, *Energy Environ. Sci*., 2012, **5**, 8726.

13. W. Wang, Q. Hao, W. Lei, X. Xia and X. Wang, *RSC Adv*., 2012, **2**, 10268.

14. M. Sawangphruk, M. Suksomboon, K. Kongsupornsak, J. Khuntilo, P. Srimuk, Y. Sanguansak, P. Klunbud, P. Suktha and P. Chiochan, *J. Mater. Chem. A***,** 2013,**1**, 9630.

15. G. A. Snook, P. Kao and A. S. Best, *J. Power Sources*, 2011, **196**, 1.

16. C. A. Amarnath, J. H. Chang, D. Y. Kim, R. S. Mane, S. H. Han, and D. Sohn, *Mater. Chem. Phys*., 2009, **113**, 14.

17. C. A. Amarnath, J. H. Chang, J. Lee, D. Y. Kim, R. S. Mane, S. H. Han and D. Sohn, *Electrochem. Solid State Lett*., 2008, **11,** A167.

18. F. Zhang, T. Zhang, X. Yang, L. Zhang, K. Leng, Y. Huang, and Y. Chen, *Energy Environ. Sci*., 2013, **6**, 1623.

19. L. L. Zhang, R. Zhou and X. S. Zhao, *J. Mater. Chem*., 2010, **20**, 5983.

20. X. Zhang, D. Zhao, Y. Zhao, P. Tang, Y. Shen, C. Xu, H. Li and Y. Xiao, *J. Mater. Chem. A*, 2013, **1**, 3706.

21. X. Wang, A. Sumboja, M. Lin, J. Yan and P. S. Lee, *Nanoscale* 2012, **4**, 7266.

22. G. A. Snook, T. L. Greaves and A. S. Best, *J. Mater. Chem*., 2011, **21**, 7622.

23. S. Chen, W. Xing, J. Duan, X. Hu and S. Z. Qiao, *J. Mater Chem. A*, 2013, **1**, 2941.

24. M. Zhi, C. Xiang, J. Li, M. Li and N. Wu, *Nanoscale*, 2013, **15**, 72.

25. S. Boukhalfa, K. Evanoff and G. Yushin *Energy Environ. Sci*., 2012, **5**, 6872.

26. W. Li, X. Yan, J. Chen, Y. Feng and Q. Xue, *Nanoscale*, 2013, **5**, 6053.

27. K. Wang, P. Zhao, X. Zhou, H. Wu and Z. Wei, *J. Mater. Chem*., 2011, **21**, 16373.

28. J. Dev, R. I. Jafri, A. K. Mishra and S. Ramaprabbhu, *J. Mater. Chem*., 2011, **21**, 17601.

29. J. Duay, E. Gillette, R. Liu and S. B. Lee, *Phys. Chem. Chem. Phys*., 2012, **14**, 3329.

30. M. Ammam and J. Fransaer, *Chem. Commun*., 2012, **48**, 2036.

31. V. L. Pushparaj, M. M. Shaijumon, A. Kumar, S. Murugesan, L. Ci, R. Vajtai, R. J. Linhardt, O. Nalamasu, and P. M. Ajayan, *Proc. Natl. Acad. Sci. U. S. A*., 2007, **104**,13574.

32. Y. Liu, Y. Zhao, B. Sun and C. Chen, *Acc. Chem. Res*., 2013, **46**, 702.

33. M. Rohwerder, S. I. Uppenkamp and C. A. Amarnath, *Electrochimi. Acta*, 2011, **56**, 1889.

34. M. S. Tamboli, M. V. Kulkarni, R. H. Patil, W. N. Gade, S. C. Navale and B. B. Kale, *Colloids and Surf. B: Biointerf*., 2012, **92**, 35.

35. P. K. Prabhakar, S. Raj, P. R. Anuradha, S. N. Sawant and M. Doble, *Colloids and Surf. B: Biointerf*., 2011, **86**, 146.

36. N. V. Ivanova, N. N. Trofimova, L. A. Es'kova, and V. A. Babkin, *Int. J. Carbohydr. Chem*. 2012, **2012**, 459410, 9 pages.

37. E. Bulut, and M. Özacar, *Ind. Eng. Chem. Res*., 2009, **48**, 5686.

38. C. A. Amarnath, J. Kim, K. Kim, J. Choi and D. Sohn, *Polymer*, 2008, **49**, 432.

39. A. Tiwari and V. Singh, *Carbohydr. Polym*., 2008, **74**, 427.

40. C. M. Correa, R. Faez, M. A. Bizeto, and F. F. Camilo, *RSC Adv*., 2012, **2**, 3088.

41. E. T. Kang, K. G. Neoh, and K. L. Tan, *Prog. Polym. Sci*., 1998, **23**, 277

42. R. Ji, W. Sun and Y. Chu, *RSC Adv*., 2014, **4**, 6055.

43. K. S. Kim, and S. J. Park, *Synth. Met*., 2012, **162**, 2107.

44. H. P. Cong, X.C. Ren, P. Wang and S. H. Yu, *Energy Environ. Sci*., 2013, **6**, 1185.

45. S. Tawde, D. Mukesh and J. V. Yakhmi, *Synth. Met*., 2002, **125**, 401.

46. J. Xu, K. Wang, S. Z. Zu, B. H. Han and Z. Wei, *ACS Nano*, 2010, **4**, 5019.

47. J. Zhang and X. S. Zhao, *J. Phys. Chem. C*, 2012, **116**, 5420.

48. V. Nandakumar, G. Suresh, S. Chittaranjan, and M. Doble, *Ind. Eng. Chem. Res*., 2013, **52,** 751.

49. L. S. A. de Melo, A. S. L. Gomes, S. Saska, K. Nigoghossian, Y. Messaddeq, S. J. L. Ribeiro, and R. E. J. de Araujo, *Fluoresc*., 2012, **22**, 1633.

50. S. Zhang, C. Du, Z. Wang, X. Han, K. Zhang, and L. Liu, *Toxicol. in Vitro*, 2013, **27**, 739.